Two-Color Theory with Novel Infrared Behavior

T. Appelquist,[1] R. C. Brower,[2] M. I. Buchoff,[3] M. Cheng,[4] G. T. Fleming,[1] J. Kiskis,[5] M. F. Lin,[6] E. T. Neil,[7, 8]
J. C. Osborn,[9] C. Rebbi,[2] D. Schaich,[10] C. Schroeder,[11] S. Syritsyn,[8] G. Voronov,[1] P. Vranas,[11] and O. Witzel[4]

(Lattice Strong Dynamics (LSD) Collaboration)

[1]*Department of Physics, Sloane Laboratory, Yale University, New Haven, Connecticut 06520, USA*
[2]*Department of Physics, Boston University, Boston, Massachusetts 02215, USA*
[3]*Institute for Nuclear Theory, Box 351550, Seattle, WA 98195-1550, USA*
[4]*Center for Computational Science, Boston University, Boston, Massachusetts 02215, USA*
[5]*Department of Physics, University of California, Davis, California 95616, USA*
[6]*Computational Science Center, Brookhaven National Laboratory, Upton, NY 11973, USA*
[7]*Department of Physics, University of Colorado, Boulder, CO 80309, USA*
[8]*RIKEN-BNL Research Center, Brookhaven National Laboratory, Upton, NY 11973, USA*
[9]*Argonne Leadership Computing Facility, Argonne, Illinois 60439, USA*
[10]*Department of Physics, Syracuse University, Syracuse, New York 13244, USA*
[11]*Lawrence Livermore National Laboratory, Livermore, California 94550, USA*

Using lattice simulations, we study the infrared behavior of a particularly interesting SU(2) gauge theory, with six massless Dirac fermions in the fundamental representation. We compute the running gauge coupling derived non-perturbatively from the Schrödinger functional of the theory, finding no evidence for an infrared fixed point up through gauge couplings $\bar{g}^2$ of order 20. This implies that the theory either is governed in the infrared by a fixed point of considerable strength, unseen so far in non-supersymmetric gauge theories, or breaks its global chiral symmetries producing a large number of composite Nambu-Goldstone bosons relative to the number of underlying degrees of freedom. Thus either of these phases exhibits novel behavior.

Introduction A new sector, described by a strongly interacting gauge theory, could play a key role in physics beyond the Standard Model. With the recent discovery of a 125 GeV Higgs-like scalar [1, 2], SU(2) vector-like gauge theories provide attractive candidates. Due to the pseudo reality of the fundamental representation of SU(2), two-color theories with N_f massless Dirac fermions in this representation have an enhanced chiral symmetry, a novel symmetry breaking pattern SU($2N_f$) → Sp($2N_f$), and, therefore, a relatively large number of Nambu-Goldstone bosons (NGB) [3, 4]. This feature has motivated SU(2)-based models of a composite Higgs boson [5, 6] and of dark matter [7–9].

These models take $N_f = 2$, but new intriguing possibilities emerge for larger N_f. With N_f just below the value at which asymptotic freedom is lost, a conformal window opens up, with the theory initially governed by a weakly-coupled infrared fixed point (IRFP). As N_f is decreased, the strength of the fixed point increases. Below some critical value N_f^c, chiral symmetry is broken and the theory confines. This critical value defines the lower edge of the conformal window [10, 11]. Knowing the extent of the window and the behavior of theories in it and near it could be crucial for building a successful model of BSM physics.

The extent of the conformal window is also interesting from a more theoretical point of view, and this is particularly true of the two-color theory. For example, a general notion about quantum field theories, as first applied to second-order phase transitions and critical phenomena, is

that the renormalization group (RG) flow toward the infrared (IR) should result in a thinning of the degrees of freedom. This can provide an important constraint on IR behavior if it can be shown that the IR count cannot exceed the UV count. One implementation of this idea, much studied recently [12, 13], defines the degree-of-freedom count through the coefficient a entering the trace of the energy momentum tensor on an appropriate space-time manifold. Although a UV-IR inequality can perhaps be proven, it does not seem to lead to useful constraints.

Another approach [14] defines the degree-of-freedom count via the thermodynamic free energy $F(T)$, using the temperature T as the RG scale. The dimensionless quantity $f(T) \equiv 90F(T)/\pi^2 T^4$ is T-independent for a free massless theory, leading to $f = 2N_V + (7/2)N_F + N_S$, where N_V, N_F, and N_S count the gauge, Dirac-fermion, and real-scalar fields. The conjectured inequality of Ref. [14] is that for an asymptotically free theory, $f_{IR} \equiv f(0) \leq f_{UV} \equiv f(\infty)$.

In the case of an IR phase with broken chiral symmetry and confinement, f_{IR} counts the number of NGBs. For a vector-like SU(N) gauge theory with $N \geq 3$ and N_f Dirac fermions, this count is $N_f^2 - 1$. Also, in the UV, $N_V = N^2 - 1$ and $N_F = NN_f$. The above inequality then demands $N_f^c < \frac{1}{4}\left(7N + \sqrt{81N^2 - 16}\right)$. This is a testable constraint, and it has been satisfied by recent lattice simulations [15]. For $N = 2$ on the other hand, the enhanced chiral symmetry, the different pattern of sym-

metry breaking, and the resultant enhanced NGB count $(2N_f^2 - N_f - 1)$ [3] lead to a significantly reduced bound on N_f for the broken phase: $N_f^c < (4 + \sqrt{30})/2 \approx 4.7$.

Crude estimates of the edge of the conformal window, based on quasi-perturbative methods, also exist. Gap-equation methods [16] provide an estimate of the gauge coupling strength, and therefore maximum value of N_f, required to induce spontaneous chiral symmetry breaking. For any $SU(N)$ gauge theory, these notions lead to the estimate $N_f^c \approx 4N$. While this is nicely compatible with the inequality for $N \geq 3$, it clearly disagrees with it for $N = 2$. This tension suggests that the $N_f = 6$ theory could be particularly worthy of study.

Early lattice calculations attempted to explore the two-color conformal window by studying the lattice theory at strong bare coupling [17, 18]. Recent efforts have primarily searched for an IRFP with non-perturbative running coupling calculations. Evidence that $N_f = 10$ ($N_f = 4$) is inside (outside) the conformal window is presented in Ref. [19]. Additionally, Ohki *et al*. argue that $N_f = 8$ is inside the conformal window [20]. The case $N_f = 6$, arguably the most interesting, while tackled by many groups [19, 21–24], has remained inconclusive.

Here we study the $N_f = 6$ theory, drawing on larger computational resources than in all previous work, to determine whether $N_f = 6$ has an IRFP by calculating the Schrödinger Functional (SF) [25] running coupling. We use the stout-smeared [26] Wilson fermion action, which suppresses coupling the fermions to unphysical fluctuations of the gauge field on the scale of the lattice spacing. This improved action reduces lattice artifacts and allows us to search for an IRFP up through a large and interesting range of running couplings. Smeared actions have also been used in SF running coupling studies of other theories [27, 28].

Preliminaries A stout-smeared fermion action replaces "thin" gauge links by "fat" links which are averaged with nearby gauge links. To define a stout-smeared [26] link is we start with $C_\mu(x)$, the weighted sum of staples about the link $(x, x + \hat{\mu})$:

$$C_\mu(x) = \sum_{\nu \neq \mu} \rho_{\mu\nu} \left(U_\nu(x) U_\mu(x + \hat{\nu}) U_\nu^\dagger(x + \hat{\mu}) \right.$$
$$\left. + U_\nu^\dagger(x - \hat{\nu}) U_\mu(x - \hat{\nu}) U_\nu(x - \hat{\nu} + \hat{\mu}) \right). \quad (1)$$

We want our fat links to be elements of $SU(N)$. This is guaranteed by taking the smearing kernel to be of form e^{iQ} with Q an element of the Lie algebra $\mathfrak{su}(N)$. We take

$$Q_\mu(x) = \frac{i}{2} \left(\Omega_\mu^\dagger(x) - \Omega_\mu(x) \right)$$
$$- \frac{i}{2N} \text{Tr} \left(\Omega_\mu^\dagger(x) - \Omega_\mu(x) \right), \quad (2)$$

with $\Omega_\mu(x) = C_\mu(x) U_\mu^\dagger(x)$ (μ is not summed over). Then a fat link is defined by

$$U_\mu^{(n+1)}(x) = \exp\left(iQ_\mu^{(n)}(x) \right) U_\mu^{(n)}(x). \quad (3)$$

This smearing procedure may be applied iteratively, say n_ρ times, to produce stout links $\tilde{U} = U^{(n_\rho)}$. It has the advantage that it is analytic and can therefore be used in conjunction with molecular dynamics (MD) updating schemes such as [29]. The formulas required to implement this smearing procedure in an MD algorithm are derived for the case of SU(3) links in [26]. We have derived the relevant formulas for the SU(2) case. Recently, another group implemented two-color stout-smearing as well [30].

We use only one level of stout-smearing with an isotropic smearing parameter $\rho_{\mu\nu} = \rho = 0.25$. As all calculations in this work are done with Dirichlet boundary conditions (BC) in the time directions, there is some ambiguity in how to implement the smearing of the gauge field near this boundary. We choose to not smear the boundary links with bulk links and *vice versa*. This choice results in a simpler running-coupling observable (which will be defined in the next section).

The Wilson fermion action contains an additional irrelevant operator that lifts the mass of the fermion doublers to the cutoff scale so they decouple from the calculation. This additional term explicitly breaks chiral symmetry, and as a result the fermion mass is additively renormalized. The bare mass m_0 therefore must be carefully tuned in order to restore chiral symmetry. The critical value of the bare mass (as a function of the bare coupling) $m_c(g_0^2)$ is defined as the bare mass value that results in a zero renormalized quark mass [31]. In practice, m_c is determined, at fixed bare gauge coupling g_0^2 and lattice volume $(L/a)^3 \times 2L/a$, as the root of a fitted linear function to measurements of the renormalized quark mass versus the bare quark mass. This is done for a range of bare couplings and lattice volumes and the results are fit to a polynomial given by

$$m_c^{\text{fit}}\left(g_0^2, \frac{a}{L} \right) = \sum_{i=1}^n g_0^{2i} \left[a_i + b_i \left(\frac{a}{L} \right) \right]. \quad (4)$$

Then, $m_c^{\text{fit}}(g_0^2, 0)$ is used in the running coupling calculations. All data used to fit $m_c^{\text{fit}}(g_0^2, a/L)$ and $m_c^{\text{fit}}(g_0^2, 0)$ are shown in Figure 1.

In order to guarantee that we can take a continuum limit, we need to obtain data only from the weak-coupling side of any spurious lattice phase transition. With this in mind, we scan through the bare parameter space and locate peaks in the plaquette susceptibility on a $L/a = 10$ lattice. This search indicates a line in the $m_0 - g_0^2$ plane of first order phase transitions that ends at a critical point at around $g_0^2 \approx 2.2$. For $g_0^2 \lesssim 2.2$, we see crossover behavior. In Figure 1, we show the above transition line plotted along with $m_c^{\text{fit}}(g_0^2, 0)$. Figure 1 indicates that our action has a sensible continuum limit only for $g_0^2 \lesssim 2.175$. Therefore, we examine the running coupling only on lattices with a bare coupling within this range.

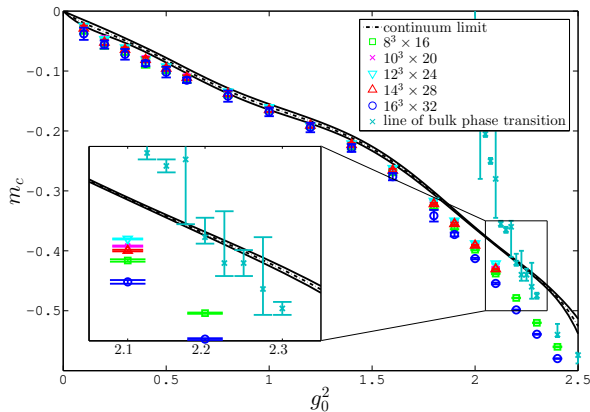***Running Coupling*** To define a non-perturbative renormalized coupling, we employ the Schrödinger

FIG. 1: Bare masses that result in zero PCAC mass at lattice volumes $8^3 \times 16$, $10^3 \times 20$, $12^3 \times 24$, $14^3 \times 28$, and $16^3 \times 32$. All data points fit to $m_c^{\text{fit}}\left(g_0^2, \frac{a}{L}\right)$ and the continuum extrapolation $m_c^{\text{fit}}\left(g_0^2, 0\right)$ (black dashed line) are shown. $m_c^{\text{fit}}\left(g_0^2, 0\right)$ determines masses used in running coupling simulations. Additionally the peak in the plaquette susceptibility (turquoise xs) is shown. We collect all running coupling data along the critical mass line on the weak coupling side of the phase transition line.

functional (SF) [25]. It is given by a path integral over gauge and fermion fields that reside within a four-dimensional Euclidean box of spatial extent L with periodic BC's in spatial directions and Dirichlet BC's in the time direction. We choose gauge BC's [32], $U\left(x, \mathrm{k}\right)|_{x^0=0} = \exp\left[-i\eta \frac{a}{L}\tau_3\right]$ and $U\left(x, \mathrm{k}\right)|_{x^0=L} = \exp\left[-i\left(\pi-\eta\right)\frac{a}{L}\tau_3\right]$, and fermion BC's [33], $P_+\psi|_{x^0=0} = \bar{\psi}P_-|_{x^0=0} = P_-\psi|_{x^0=L} = \bar{\psi}P_+|_{x^0=L} = 0$. These BC's classically induce a constant chromoelectric background field whose strength is characterized by the dimensionless parameter η. With these BC's the SF is given by $\mathcal{Z}(\eta, L) = \int D\left[U, \psi, \bar{\psi}\right] e^{-S[U, \psi, \bar{\psi}; \eta]}$.

The running coupling is then defined by,

$$\frac{k}{\bar{g}^2\left(g_0^2, \frac{L}{a}\right)} = \left.\frac{\partial}{\partial\eta}\log\mathcal{Z}\right|_{\eta=\pi/4} = \left\langle\frac{\partial S}{\partial\eta}\right\rangle, \quad (5)$$

with $k = -24\left(L/a\right)^2\sin\left[\left(a/L\right)^2\left(\pi/2\right)\right]$ so that the renormalized coupling agrees with the bare coupling at tree-level. The first two perturbative coefficients of the SF beta function are the universal coefficients given in [10]. This renormalization scheme has the virtue that it is fully non-perturbative and it is amenable to a lattice calculation.

We calculate the SF renormalized coupling over a range of bare couplings and lattice volumes. Lattice perturbation theory gives $g_0^2/\bar{g}^2$ as an expansion in powers of g_0^2. This motivates an interpolating fit [34],

$$\frac{1}{g_0^2} - \frac{1}{\bar{g}^2\left(g_0^2, \frac{L}{a}\right)} = \sum_{i=0}^{N_{L/a}} a_{i,L/a} g_0^{2i}. \quad (6)$$

We choose the lowest possible $N_{L/a}$ to give a reasonable χ^2 per dof (in practice, values in the range $\chi^2/\mathrm{dof} \in [0.7, 1.5]$), finding $N_{L/a\leq 12} = 6$ and $N_{L/a>12} = 5$. This procedure produces smooth functions, one for each lattice volume L/a, of the renormalized coupling versus the bare coupling. Before using this interpolation for further analysis, it is worth noting that there is no hint of an IRFP in the lattice data and therefore in the interpolating curves. At any fixed g_0^2, the running coupling $\bar{g}^2\left(g_0^2, \frac{L}{a}\right)$ is seen only to increase as a function of L/a in the range of the data.

The question is whether a careful continuum extrapolation will indicate otherwise. A step scaling [35] analysis allows us to address this issue and to study the renormalized coupling over a large range of scales in computationally feasible manner. The continuum step scaling function $\sigma\left(u, s\right)$ is defined by

$$\int_u^{\sigma(u,s)} \frac{d\bar{g}^2}{\beta\left(\bar{g}^2\right)} = 2\log s. \quad (7)$$

It is the renormalized coupling at a length scale sL given that the running coupling $\bar{g}^2 = u$ at a length scale L. On the lattice we calculate the discrete step scaling function,

$$\Sigma\left(u, \frac{a}{L}, s\right) \equiv \left.\bar{g}^2\left(g_{0*}^2, \frac{sL}{a}\right)\right|_{\bar{g}^2\left(g_{0*}^2, \frac{L}{a}\right)=u}. \quad (8)$$

It is the value of the renormalized coupling on a lattice volume of $(sL/a)^4$ and bare coupling tuned such that we have a renormalized coupling of u on a lattice of volume $(L/a)^4$. We arrive back at a continuum step scaling function by taking the continuum limit:

$$\sigma\left(u, s\right) = \lim_{a/L\to 0} \Sigma\left(u, \frac{a}{L}, s\right). \quad (9)$$

From here we use $s = 2$ and drop reference to this from our notation.

To extract σ as a function of u, we first use the interpolating fits, given by Eq. 6, to evaluate Σ at each fixed value of u and $L/a = 5$, 6, 7, 8, 9, 10, and 12. We take the continuum limit, at each u independently, by fitting $\Sigma\left(u, a/L\right)$ to a polynomial in a/L, and extrapolating to $a/L \to 0$. Our result, shown in Fig 2, displays several plots of the quantity $\left(\sigma\left(u\right) - u\right)/u$ versus u. This quantity is a finite-difference version of the continuum beta function. In one curve (red), we fit $\Sigma\left(u, a/L \leq 1/6\right)$ to a quadratic polynomial and then extrapolate the result to $a/L \to 0$. Additionally, we show, $\Sigma\left(u, a/L \leq 1/5\right)$ extrapolated from a cubic polynomial fit (green). We see that these two curves are consistent, but the errors of the cubic extrapolation become large at $u \approx 8$. The remaining (blue) curve is obtained with a constant extrapolation to the continuum using only the three points with $a/L \leq 1/9$.

To asses the goodness-of-fit of any particular functional form for continuum extrapolation of Σ we examine χ^2/dof over the entire range of u. For the constant extrapolation (blue) in Fig. 2 for $L/a \geq 9$, χ^2/dof varies from 0.5-2.
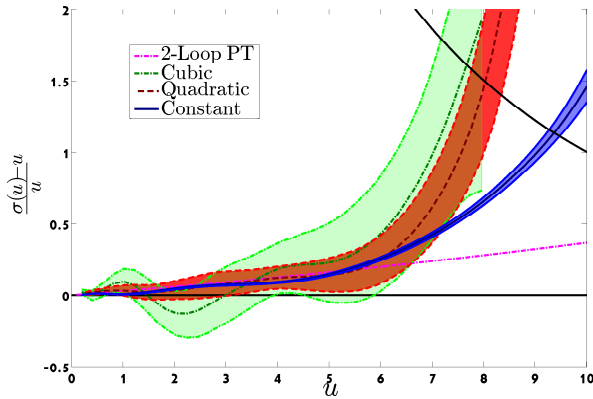
FIG. 2: $(\sigma(u) - u)/u$ vs u for three different extrapolations to the continuum. A contour at $\bar{g}^2 = 20$ is shown to provide a measure of the strength of renormalized coupling explored here. The 2-loop perturbative result is also shown here (dot-dashed magenta).

A quadratic extrapolation (red) for $L/a \geq 6$ and a cubic extrapolation for $L/a \geq 5$ have comparable χ^2/dof ranging from 0.5-4 throughout the range of u. The constant (quadratic and cubic) extrapolation relies on fits with two (three) degrees-of-freedom.

These various extrapolations all perform well at reproducing the perturbative two-loop curve (magenta) at small values of u. If the resulting curves were to cross zero at some larger u, this would be indicative of an IRFP. We see no indication of this; in fact we see, regardless of which extrapolation we use, the running coupling grow up to and beyond estimates of the critical coupling required to induce spontaneous chiral symmetry breaking [16]. We see no evidence even of an inflection point, which would hint at an IRFP at a stronger coupling strength.

We next compare these three continuum extrapolations more carefully and comment also on extrapolation via a linear polynomial in a/L. For each u, $\Sigma(u, a/L)$, evaluated at $L/a = 5$, 6, 7, 8, 9, 10, and 12, is fit to a cubic polynomial, $p(a/L) = \sum_{i=0}^{3} \alpha_i (a/L)^i$. For several values of a/L, the relative sizes of the constant, $O(a/L)$, $O(a/L)^2$, and $O(a/L)^3$ terms in the polynomial are plotted vs u. We can then assess the validity of some truncation of the polynomial continuum extrapolation within some window in a/L. We show the results of such an analysis in Fig. 3 for $L/a = 6$, 9, and 12. A number of interesting features are evident. At weak coupling the lattice artifacts are small, and a constant extrapolation adequately describes the continuum limit. But at intermediate and strong coupling ($u \gtrsim 6$), lattice artifacts become significant. Throughout the coupling range, the linear and quadratic lattice artifacts are comparable for $a/L \geq 1/9$ and hence we can not perform a reliable linear extrapolation to the continuum. The cubic contribution, however,
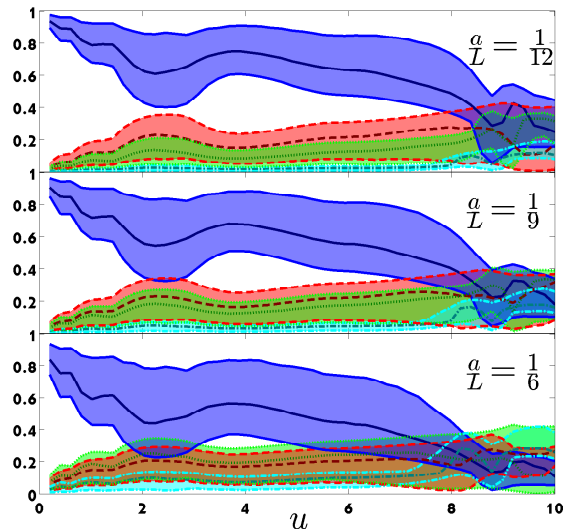

FIG. 3: Plots of relative magnitudes of low order contributions to the continuum extrapolation. We fit $s = 2$ steps at $L/a = 5$, 6, 7, 8, 9, 10, and 12 to a polynomial $\sum_{i=0}^{3} \alpha_i \left(\frac{a}{L}\right)^i$. Then $|\alpha_0|/T$ (blue), $\left|\alpha_1 \left(\frac{a}{L}\right)\right|/T$ (red), $\left|\alpha_2 \left(\frac{a}{L}\right)^2\right|/T$ (green), and $\left|\alpha_3 \left(\frac{a}{L}\right)^3\right|/T$ (cyan) are plotted versus u, at various values of a/L, with $T = \sum_{i=0}^{3} \left|\alpha_i \left(\frac{a}{L}\right)^i\right|$.

is small for $a/L \leq 1/6$ and $u \lesssim 8$, indicating that a quadratic extrapolation to the continuum is reliable at least up to this input coupling strength. This indicates that the running coupling reaches a $\bar{g}^2$ of order 20 without encountering an IRFP.

Insight may also be gleaned by plotting the extrapolation to the continuum at fixed coupling strength u. We show in Fig. 4 the example of $u = 7.5$. We plot $\Sigma(u, a/L)$ vs a/L, along with a quadratic and cubic polynomial fit, as well as a constant extrapolation based on the three smallest a/L values. These correspond to the fits used in Fig. 2. Fig. 4 demonstrates that a constant extrapolation to the continuum is reasonable. Taking the larger a/L points into account shows the presence of significant non-linear lattice artifacts, in fact suggesting that the constant extrapolation significantly underestimates $\sigma(u)$ for $u \gtrsim 7$. It is also evident that the quadratic and cubic fits extrapolate to a value of σ that is well above the smallest-a/L points. It is likely that the true extrapolated value is somewhere between the constant and quadratic extrapolations.

Recently Hayakawa *et al.* claim to see evidence of an IRFP in the two-color six-flavor theory [24]. They employ the SF method as we do but with the unimproved Wilson fermion action and a linear extrapolation to the continuum. It is reasonable to expect that for large enough L/a the linear term will be the dominant lattice artifact but it is difficult to quantify how large an L/a is necessary outside of perturbation theory. Other extrapolation forms, including
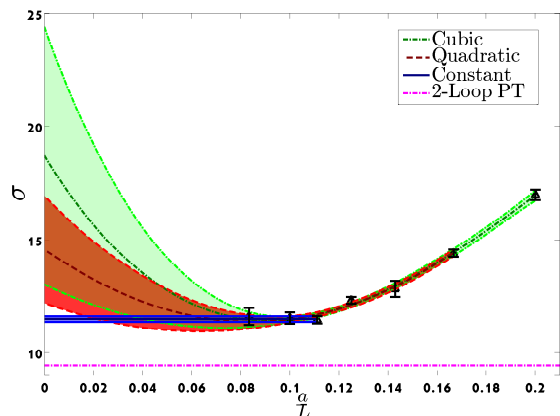
FIG. 4: Plot of $\Sigma\left(u=7.5,a/L\right)$ vs a/L with various extrapolations to the continuum. The continuum limit of the quantity is obtained by fitting these points to a polynomial in a/L.

quadratic terms can be used to fit their data with a comparable or slightly better χ^2/dof. When this is done, we cannot conclude that an IRFP exists. Moreover, from *our* data set, sampling many more bare couplings and lattice volumes, we are able to study the relative contributions of different lattice artifacts. In Figure 3, we see that in the strong coupling regime, the quadratic term becomes significant in the a/L range studied by Hayakawa *et al*. and by us. With the caveat that we use a different lattice action, the relative importance of the quadratic term suggests that concluding the existence of an IRFP from a linear extrapolation to the continuum is premature.

To summarize, for an SU(2) gauge theory with six massless fermions in the fundamental representation, we find no evidence of an infrared fixed point in the running gauge coupling as defined in the Schrödinger Functional scheme. Our simulations reach well into a strong-coupling range, potentially capable of triggering chiral symmetry breaking and confinement. We conclude that this theory either flows to a very strong infrared fixed point, so-far unseen in non-supersymmetric theories, or it breaks chiral symmetry and confines, producing a large number (65) of Nambu-Goldstone bosons, well above the number of underlying fermionic and gauge degrees of freedom. Thus either of these (zero-temperature) phases exhibits novel behavior. In the latter case, the finite-temperature phase transition can be expected to have interesting features. We could in principle probe even larger couplings than presented here, but the computational challenges and lattice-artifact difficulties grow with coupling strength. Other approaches, such as the computation of correlation functions and the particle spectrum, will be important to firmly establish the infrared nature of this theory.

[1] G. Aad et al. (ATLAS Collaboration), Phys.Lett. **B716**, 1 (2012), 1207.7214.
[2] S. Chatrchyan et al. (CMS Collaboration), Phys.Lett. **B716**, 30 (2012), 1207.7235.
[3] M. E. Peskin, Nucl.Phys. **B175**, 197 (1980).
[4] J. Preskill, Nucl. Phys. **B177**, 21 (1981).
[5] J. Galloway, J. A. Evans, M. A. Luty, and R. A. Tacchi, JHEP **1010**, 086 (2010), 1001.1361.
[6] E. Katz, A. E. Nelson, and D. G. Walker, JHEP **0508**, 074 (2005), hep-ph/0504252.
[7] R. Lewis, C. Pica, and F. Sannino, Phys.Rev. **D85**, 014504 (2012), 1109.3513.
[8] A. Hietanen, R. Lewis, C. Pica, and F. Sannino (2013), 1308.4130.
[9] M. R. Buckley and E. T. Neil, Phys.Rev. **D87**, 043510 (2013), 1209.6054.
[10] W. E. Caswell, Phys.Rev.Lett. **33**, 244 (1974).
[11] T. Banks and A. Zaks, Nucl.Phys. **B196**, 189 (1982).
[12] J. L. Cardy, Phys.Lett. **B215**, 749 (1988).
[13] Z. Komargodski and A. Schwimmer, JHEP **1112**, 099 (2011), 1107.3987.
[14] T. Appelquist, A. G. Cohen, M. Schmaltz, and R. Shrock, Phys.Lett. **B459**, 235 (1999), hep-th/9904172.
[15] E. T. Neil, PoS **Lattice 2011**, 009 (2011), 1205.4706.
[16] A. G. Cohen and H. Georgi, Nucl.Phys. **B314**, 7 (1989).
[17] Y. Iwasaki, K. Kanaya, S. Kaya, S. Sakai, and T. Yoshie, Phys.Rev. **D69**, 014507 (2004), hep-lat/0309159.
[18] K.-i. Nagai, M. G. Carrillo-Ruiz, G. Koleva, and R. Lewis, PoS **LATTICE2010**, 065 (2010), 1011.0805.
[19] T. Karavirta, J. Rantaharju, K. Rummukainen, and K. Tuominen, JHEP **1205**, 003 (2012), 1111.4104.
[20] H. Ohki, T. Aoyama, E. Itou, M. Kurachi, C.-J. D. Lin, et al., PoS **LATTICE2010**, 066 (2010), 1011.0373.

[21] F. Bursa, L. Del Debbio, L. Keegan, C. Pica, and T. Pickup, Phys. Lett. **B696**, 374 (2011), 1007.3067.

[22] G. Voronov, PoS **LATTICE2011**, 093 (2011), 1301.4141.

[23] G. Voronov, PoS **LATTICE2012**, 039 (2012), 1212.1376.

[24] M. Hayakawa, K. I. Ishikawa, S. Takeda, and N. Yamada (2013), 1307.6997.

[25] M. Luscher, R. Narayanan, P. Weisz, and U. Wolff, Nucl.Phys. **B384**, 168 (1992), hep-lat/9207009.

[26] C. Morningstar and M. J. Peardon, Phys.Rev. **D69**, 054501 (2004), hep-lat/0311018.

[27] T. DeGrand, Y. Shamir, and B. Svetitsky, Phys. Rev. **D82**, 054503 (2010), 1006.0707.

[28] T. DeGrand, Y. Shamir, and B. Svetitsky (2013), 1307.2425.

[29] S. A. Gottlieb, W. Liu, D. Toussaint, R. Renken, and R. Sugar, Phys.Rev. **D35**, 2531 (1987).

[30] S. Catterall and A. Veernala (2013), 1303.6187.

[31] M. Luscher, S. Sint, R. Sommer, P. Weisz, and U. Wolff, Nucl.Phys. **B491**, 323 (1997), hep-lat/9609035.

[32] M. Luscher, R. Sommer, U. Wolff, and P. Weisz, Nucl.Phys. **B389**, 247 (1993), hep-lat/9207010.

[33] S. Sint, Nucl.Phys. **B421**, 135 (1994), hep-lat/9312079.

[34] T. Appelquist, G. T. Fleming, and E. T. Neil, Phys.Rev. **D79**, 076010 (2009), 0901.3766.

[35] M. Luscher, P. Weisz, and U. Wolff, Nucl.Phys. **B359**, 221 (1991).

[36] R. G. Edwards and B. Joo (SciDAC Collaboration, LHPC Collaboration, UKQCD Collaboration), Nucl.Phys.Proc.Suppl. **140**, 832 (2005), hep-lat/0409003.